Characterisation of the fumarate hydratase repertoire in *Trypanosoma cruzi*

Ricardo A. P. de Pádua[*†], Ali Martin Kia[†], Antonio José Costa Filho[§], Shane R. Wilkinson[†1], M. Cristina Nonato[*1]

[*]Laboratório de Cristalografia de Proteínas de Ribeirão Preto, Faculdade de Ciências Farmacêuticas de Ribeirão Preto – Universidade de São Paulo, 14040-903, Ribeirão Preto, SP, Brazil,

[†]School of Biological and Chemical Sciences, Queen Mary University of London, Mile End Road, London E1 4NS, United Kingdom,

[§]Laboratório de Biofísica Molecular, Faculdade de Filosofia, Ciências e Letras de Ribeirão Preto – Universidade de São Paulo, 14040-901, Ribeirão Preto, SP, Brazil

[1] To whom correspondence should be addressed (enzyme work: email cristy@fcfrp.usp.br, parasite work: s.r.wilkinson@qmul.ac.uk).

Abstract

Nifurtimox and benznidazole represent the only treatments options available targeting Chagas disease, the most important parasitic infection in the Americas. However, use of these is problematic as they are toxic and ineffective against the more severe stages of the disease. In this work, we used a multidisciplinary approach to characterise the fumarases from *Trypanosoma cruzi*, the causative agent of Chagas Disease. We showed this trypanosome expresses cytosolic and mitochondrial fumarases that *via* an iron-sulfur cluster mediate the reversible conversion of fumarate to S-malate. Based on sequence, biochemical properties and co-factor binding, both *T. cruzi* proteins share characteristics with class I fumarases, enzymes found in bacteria and some other protozoa but absent from humans, that possess class II isoforms instead. Gene disruption suggested that although the cytosolic or mitochondrial fumarase activities are individually dispensable their combined activity is essential for parasite viability. Finally, based on the mechanistic differences with the human (host) fumarase, we designed and validated a selective inhibitor targeting the parasite enzyme. This study showed that *T. cruzi* fumarases should be exploited as targets for the development of new chemotherapeutic interventions against Chagas disease.

Key words: *Trypanosoma cruzi*; gene disruption; tricarboxylic acid cycle; drug design; enzyme inhibitor; iron-sulfur protein

1. Introduction

Throughout Latin America approximately 8 million people suffer from Chagas disease, a neglected tropical infection caused by the flagellated protozoan parasite *Trypanosoma cruzi* (World Health Organization, 2013). This disease is characterised by a series of life-threatening mega syndromes that promote damage to the heart, intestines and central nervous system, severely affecting the quality of life of infected patients [1].

The normal route of transmission of this zoonotic infection is *via* the hematophagous behaviour of insects belonging to the Reduviidae family, in which part of *T. cruzi*'s life cycle occurs, to humans, where the cycle is completed [2]. However, as a result of alternative modes of transmission such as through blood transfusions, organ transplantation, congenital and ingestion of contaminated food [3], and population migration, Chagas disease has started to emerge as a public health problem at non-endemic sites such as the USA and Europe [4].

Benznidazole and nifurtimox currently represent the only treatment options available against Chagas disease but their use is controversial. They are highly toxic and not effective in curing the infection during the lethal disease staging while some strains are refractory to treatment. In addition, the drug regimens are prolonged with a course of treatment requiring multiple daily doses taken over a 1 to 4 month period. Often, the recommended schedules are not completed, usually because of their side effects, resulting in considerable scope for the development of resistance. There is a considerable need for novel therapeutic strategies targeting Chagas disease and exploring the biochemistry of *T. cruzi* is seen as an important strategy to identify and validate new drug targets for the development of innovative treatments [5].

Fumarases (EC 4.2.1.2), also known as fumarate hydratases, are ubiquitous enzymes that catalyse the reversible conversion of fumarate to L-malate [6]. Based on sequence, structure, biochemical

properties and co-factors, they can be divided into three distinct types [7]. Class I fumarases primarily expressed by bacteria and some protozoa, are homodimeric iron-sulfur (4Fe-4S) containing enzymes of approximately 120 kDa in size, and are readily inactivated by superoxide anions, heat or radiation. In contrast, class II fumarases are homotetrameric, iron independent proteins of approximately 200 kDa in size that are expressed by bacteria and numerous eukaryotes including higher plants, fungi and mammals [8]. Higher eukaryotic cells express one class II enzyme that is dual localized by reverse translocation after undergoing proteolytic processing to generate different echoforms [9-11]. One of these forms is localized to the mitochondrion where it participates in the Kreb's cycle while the second, located in the cytosol, plays a role in amino acid and fumarate metabolism. Intriguingly, the cytosolic variant is postulated to participate in the cellular response to DNA double strand breaks with this enzyme undergoing transport into the nucleus [12]. A third fumarase class has been identified from prokaryotes. This enzyme is composed of a heterodimer with an alpha and a beta subunit resembling the N-terminal and C-terminal parts of class I fumarase, respectively [13, 14].

Analysis of the trypanosomal databases has shown that trypanosomes have the potential to express two class I fumarases, enzymes that are completely distinct from the class II counterparts found in humans. This, coupled with the observation that the total fumarase activity in an insect-stage *Trypanosoma brucei* cell is essential for parasite viability [15], prompted us to evaluate whether these enzymes constitute anti-chagasic drug targets. Here, we show that the total fumarase activity is important, if not essential, for *T. cruzi* viability and that both *T. cruzi* enzymes catalyse the reversible conversion of fumarate to L-malate with this activity being readily inhibited by the sulfur-containing malate derivative, thiomalate. Our results suggest that fumarase could be exploited as a potential drug target in *T. cruzi* and thus selective inhibiton of fumarase may constitute a new strategy against Chagas disease.

2. Materials and Methods

2.1 Cell culturing

T. cruzi epimastigote Sylvio X.10.6 were grown at 28°C in RPMI 1640 medium supplemented with 5 g L^{-1} trypticase, 20 mM HEPES pH 7.5, 10 % (v/v) heat-inactivated calf fetal serum, 0.22 g L^{-1} sodium pyruvate, 0.34 g L^{-1} sodium glutamate, 2500 U L^{-1} penicillin, 0.25 g L^{-1} streptomycin and 20 mg L^{-1} hemin. DNA was introduced into *T. cruzi* epimastigotes using the Human T-cell Nucleofector® kit and an Amaxa® Nucleofector™ (Lonza AG) set to program X-001. Transformed parasites were grown in the presence of 5 or 10 µg mL^{-1} puromycin, 5 or 10 µg mL^{-1} blasticidin, 5 µg mL^{-1} hygromycin and/or 100 µg mL^{-1} G418.

T. cruzi amastigote parasites were grown in African green monkey kidney epithelial (Vero) cells at 37 °C in a 5% (v/v) CO_2 atmosphere in RPMI 1640 medium. Uninfected Vero cells were maintained in this medium and sub-cultured following trypsin treatment. To produce *T. cruzi* metacyclic cells, epimastigote cultures were allowed to grow to late stationary phase resulting in differentiation of the parasite. These were used to infect Vero cells. Following overnight incubation at 37 °C in a 5% (v/v) CO_2 atmosphere, non-internalized parasites were removed by washing in liver infusion tryptose medium containing non-inactivated fetal calf serum. Bloodstream form metacyclics emerged 10 days after the initial infection and used to infect new Vero cells at a ratio of 10 parasites per mammalian cell. After 2 days, the medium was aspirated and the cells examined microscopically following Giemsa staining. The percentage of infected Vero cells and the number of amastigotes per infected cell were determined by analyzing 100 host cells randomly distributed across several fields of view. The mean number of parasites found in all host cells (mean abundance) was calculated using the quantitative software (QPweb 1.0) with 95% confidence interval by the bias-corrected and accelerated (BCa) bootstrap method with 2000 bootstrap replications.

2.2 Protein purification

The vectors used to express various fumarases in *E. coli* were generated as follows: full length Tc*fhc* was amplified from *T. cruzi* genomic DNA (gDNA) with the primers gaattcATGAGTCTGTGCGAAAACT and gcggccgcATCAAAGGAGTTTGGAAAAAAAG (lower case correspond to restriction sites incorporated into the primers to facilitate cloning). The amplicon was digested with *Eco*RI and *Not*I then cloned into the corresponding sites of the pET-28a vector (Novagen). The fumarase gene was subcloned into pET-28a-SUMO [16] using *Eco*RI and *Xho*I such that a DNA sequence gene coding for a hexahistidine-tagged SUMO was inserted in-frame at the 5' end of the Tc*fhc*-derived DNA fragment. For TcFHm heterologous expression, the full length Tc*fhm* gene was amplified from *T. cruzi* gDNA with the primers ggatccATGCTGCGCCGTTCTGC and gcggccgcagcaTTGGACTCATTTGAGCTG, the resultant fragment digested with *Bam*HI and *Not*I, and cloned into the corresponding sites in pET-28a-SUMO. The human fumarase gene (Hs*fh*) was subcloned from the pET-28a-*HsFH* construct [17] into pET-28a-SUMO using *Bam*HI and *Xho*I restriction sites.

Overnight cultures of *E. coli* BL21 (DE3) harboring a pET-28a-SUMO vector containing the fumarase genes were diluted 1:100 in Lysogeny Broth containing 30 μg mL^{-1} kanamycin and grown at 37 ^{o}C with aeration until the culture reached the logarithmic phase of growth (OD_{600nm} ~ 0.5-0.6). *E. coli* cultures were transferred to 18°C for 30 min and protein expression induced by addition of β-D-thiogalactopyranoside (IPTG) (TcFHc: 5 μM; TcFHm: 50 μM; HsFH: 500 μM). Cultures were incubated at 16°C for a further 24 hours before harvesting the cell. For expression of the *T. cruzi* enzymes, 200 mg L^{-1} ferrous sulfate heptahydrate, 200 mg L^{-1} ferric citrate and 2 mM cysteine were added to the growth medium. All subsequent purification steps were performed under anaerobic conditions. The cells were resuspended in buffer A (50 mM NaH_2PO_4, pH 8.5, 300 mM NaCl, 10 mM imidazole) containing 1 mM phenylmethylsulfonyl fluoride then disrupted by sonication using

10 x 30 s pulses on ice. The clarified lysate was passed through a Ni-NTA resin (Qiagen) equilibrated with buffer A. The resin was washed with the same buffer containing 25 mM imidazole and then re-equilibrated with buffer A. The histidine tagged protease ULP1 (500 µg) was added to the resin, the column incubated overnight at 8 °C. Tag-free enzymes were then eluted off the column with buffer A. Enzymes were concentrated and dialyzed against the storage buffer (50 mM Tris pH 8.5, and 150 mM NaCl) using an ultra-filter unit with 30 kDa cutoff (Amicon-Millipore).

Size exclusion chromatography of TcFHc was carried out using an isocratic run (50 mM Tris pH 8.5, 600 mM NaCl, 10 mM imidazole and 1 mM DTT) in a Superdex 200 10/300 (GE Life Sciences). The oligomeric state was estimated using molecular weight markers according to the column manufacturer's instructions.

2. 3 Enzyme kinetics

TcFHc and TcFHm activities were monitored under anaerobic conditions by following the change in absorbance at 250 nm due to consumption or formation of fumarate (ε_{250nm}=1.45 mM^{-1} cm^{-1} [18]). A reaction mixture containing 50 mM Tris pH 8.5, 150 mM NaCl, fumarate (500, 250, 125, 62.5 and 31.25 µM) or malate (8, 4, 2, 1, and 0.5 mM) was incubated at 25 °C. The background rate of fumarate consumption/formation was determined and the reaction initiated by addition of fumarase (10 µg mL^{-1}). The protein amount used was corrected based on the iron-sulfur content measured spectrophotometrically (ε_{410nm}= 15,000 $M^{-1}cm^{-1}$ [19]). Initial reaction rates were plotted versus substrate concentration and the Hill model used to fit the data by nonlinear regression in Origin (OriginLab, Northampton, MA).

2.4 Inhibition studies

The effect of thiomalate (Sigma) on the initial reaction rates of TcFHc and HsFH was assessed. TcFHc activity in 50 mM Tris pH 8.5, 150 mM NaCl buffer was followed in varying amounts of L-malate (8, 4, 2, 1, and 0.5 mM) and different thiomalate concentrations (12.86, 4.5, 1.58, 0.55 and 0 μM). Data were fitted using competitive, non-competitive and uncompetitive models by non-linear regression using GraphPad Prism software version 5.00 and the best model was selected based on the Akaike information criterion (AICc). For HsFH, activity was monitored in buffer 50 mM Tris pH 8.5, 150 mM NaCl using 50 mM L-malate with different thiomalate concentrations (200, 100, 50, 25, 12.5 and 6.25 mM). Activity was expressed as percentage of the maximum activity achieved in absence of inhibitor.

Inhibition of TcFHc using different compounds possessing free thiol groups was also tested. In these assays activity was evaluated in buffers containing 50 mM Tris pH 8.5, 150 mM NaCl and 8 mM L-malate in presence of different concentrations (50 mM, 10 mM, 2 mM, 400 μM, 80 μM, 16 μM, 3.2 μM, 640 nM and 128 nM) of β-mercaptoethanol (BME), cysteine (Cys), reduced glutathione (GSH), dithiotreitol (DTT) and sodium meso-2,3-dimercaptosuccinate (DMSA).

2.5 Electron paramagnetic resonance

EPR measurements were performed to assess the presence of an iron-sulfur cluster in TcFHc and TcFHm. A Bruker Elexsys E580 spectrometer operating at X band (9.5 GHz) equipped with a rectangular cavity was utilized. The optimal temperature for the experiments, around that of liquid helium (4-10 K), was reached using an Oxford ITC 503 cryostat. The parameters were optimized to avoid signal saturation and distortion with the final values: 10 mW microwave potency, 0.2 mT magnetic field modulation and 100 kHz magnetic field modulation frequency. Samples contained 87 μM of protein in a total volume of 50 μL.

2.6 Localization studies

To express an epitope tagged version of TcFHm the corresponding open reading frame minus its STOP codon was amplified from *T. cruzi* gDNA using the primers gaattcATGCTGCGCCGTTCTGCGGCA and gatatcTTTGAGCTGTTGGAAGAAGTC. The resultant product was digested with *Eco*RI and *Eco*RV and cloned into the corresponding site of pTEX-Tc*ntr*-9e10 [20], replacing the Tc*ntr* gene. The cloning was carried out such that the DNA sequence coding for the c-myc(9e10) epitope was inserted in-frame at the 3' end of the Tc*fhm*-derived DNA fragment. The construct was then introduced into *T. cruzi* epimastigotes by electroporation.

T. cruzi harboring pTEX-Tc*fhm*9e10 were subject to subcellular fractionation following treatment with digitonin. Parasites (4 x 10^9 cells) in logarithmic phase of growth were washed twice and resuspended in ice cold buffer D (20 mM Tris-HCl pH 7.2, 225 mM sucrose, 20 mM KCl, 10 mM KH_2PO_4, 1 mM EDTA, 5 mM MgCl) containing protease inhibitor cocktail (Roche). An aliquot of cells were lysed with an each volume of 0.2 % (v/v) Triton X-100, 300 mM NaCl and the total protein concentration determined using a Pierce BCA Protein Assay Kit (ThermoScientific). The remainder of the suspension was diluted such that when lysed a final protein concentration of 3 mg mL^{-1} was achieved. Aliquots of the suspension were mixed with 2 volumes of buffer D containing different concentrations of digitonin, incubated for 5 minutes at 28 °C, the samples clarified and supernatants collected. Equal volumes of each sample were then SDS-PAGE fractionated and analyzed by western blot analysis using antibodies raised against c-Myc(9e10) (Santa Cruz Biotechnology) as TcFHm marker and *T. brucei* enolase, *T. brucei* aldolase and *T. brucei* acetyl:succinate CoA transferase as cytosol, glycosomal and mitochondrial markers, respectively. A total lysis control sample obtained by incubating cells with 0.1 % (v/v) Triton X-100 for 20 min at 4 °C was examined in parallel.

For confocal-based localization studies the Tc*fhm and* Tc*fhc* open reading frames minus their STOP codons were amplified from *T. cruzi* gDNA using the primers actagtATGAGT

CTGTGCGAAAACTGC and gtcgacAGGAG TTTGGAAAAAAAGTCA (for Tc*fhc*) or actagtATGCTGCGCCGTTCTGCGGCA and gtcgacTTGAGCTGTTGGAAGAAGTCA (for Tc*fhm*). Fragments were digested with *Spe*I and *Sal*I and cloned into the corresponding sites of pTEX-eGFP [21]. The cloning was carried out such that the DNA sequence coding for the green fluorescence protein (GFP) was inserted in-frame at the 3' end of the Tc*fhm*- or Tc*fhc*-derived DNA fragments. *T. cruzi* epimastigotes expressing TcFHm-GFP (5 x 10^6 mL^{-1}) were suspended in medium containing 100 nM Mitotracker® Red CMXRos (Molecular Probes) and incubated at 37°C for 5 min. These cells along with parasites expressing TcFHc-GFP were washed twice in PBS, fixed in 2 % (w/v) paraformaldehyde/PBS, then washed again in PBS. Aliquots of the cell suspension (10^5 cells) were air-dried onto microscope slides, the parasite genomes stained with 200 pM 4',6-diamidino-2-phenylindole (DAPI) in 50% glycerol/PBS (Sigma-Aldrich) and slides were viewed by using a Zeiss LSM 510 confocal microscope.

2.7 Gene disruption

The constructs used to disrupt the *T. cruzi* fumarase genes were generated as follows: Primers were designed to amplify 450 or 471 bp fragments from the 5' and 3' region of the Tc*fhc* gene, respectively. These were cloned sequentially either side of a puromycin- (*pac*) or blasticidin- (*bla*) containing resistance cassette. Similarly, primers to designed to amplify 490 and 484 bp DNA fragments from the 5' and 3' region of the Tc*fhm* gene, respectively. These were cloned sequentially either side of a *pac*-, *bla*-, neomycin- (*neo*) or hygromycin- (*hyg*) containing resistance cassette. Constructs were linearized (*Sac*I/*Kpn*I for the *pac, hyg* and *neo* vectors or *Sac*II/*Kpn*I for the *bla* vector) then introduced into *T. cruzi* epimastigotes by electroporation. Integration of the DNA constructs into the *T. cruzi* genome results in deletion of ~50% of Tc*fhc* or Tc*fhm* coding sequence.

3. Results

3.1 Trypanosoma cruzi enzymes display type I fumarase characteristics

Two ORFs in the *T. cruzi* genome database [22] were identified as having potential to encode for 62 kDa proteins related to fumarase enzymes. One 1698 bp sequence (TcCLB.507257.60) located on chromosomes 36 was designated as Tc*fhc* and the second 1668 bp ORF (TcCLB.507669.10) found on chromosomes 26 was designated as Tc*fhm*. The deduced amino acid sequence of the two *T. cruzi* fumarases share 61% identical residues to each other with most of the differences found in their amino termini, and shared 75 to 82% identical residues to their *T. brucei* and Leishmanial orthologues, respectively. When TcFHc and TcFHm were compared to fumarases from other organisms they exhibited significant identity (~60%) to the class I enzymes from unicellular eukarytotes and bacteria and no similarity to the class II fumarases present in higher eukarytotes such as humans.

To facilitate their biochemical characterisation TcFHc and TcFHm were expressed as 6x(His)-SUMO amino termini tagged proteins in *E. coli*, affinity purified on a Ni^{2+} column and eluted off the matrix following cleavage with the ULP1 protease, releasing the untagged fumarase (Figure 1A). To determine its oligomeric state, purified TcFHc was subjected to size exclusion chromatography, eluting off the column as a size peak of ~147 kDa (Figure 1B). This is close to the expected size of a dimeric protein (124 kDa), in agreement to the quaternary structure reported for class 1 fumarases [7]. To investigate co-factor binding the EPR profiles of TcFHc and TcFHm were assessed (Figure 1C and D). The resultant spectra contain resonances centered on g~2.019 typical of S=1/2 spin system in an axial local symmetry. This pattern type was assigned to $[3Fe\text{-}4S]^{+}$ clusters likely produced by the oxidation of [4Fe-4S] clusters [23-26]. [4Fe-4S] clusters are described to be crucial to class I fumarases catalytic mechanism where they behave as a Lewis acid that activates the substrates [13, 14, 23, 27]. Based on their sequence, oligomeric state and co-factor binding, TcFHc and TcFHm

clearly show all the characteristics of the class I group of fumarases, distinct from their human counterparts.

3.2 Trypanosoma cruzi expresses two functional fumarases

In other organisms fumarases catalyse the reversible hydration/dehydration of fumarate/malate. To determine whether the trypanosomal enzymes could perform these reactions, the ability of purified TcFHc and TcFHm to convert fumarate to malate (hydration) and malate to fumarate (dehydration) was monitored by following the change in absorbance at 250 nm. Initial assays conducted under anaerobic conditions and using fix amount of substrate (1 mM) revealed that both parasite enzymes could readily catalyse the above reactions with an optimal pH of 8.0 to 9.0. To study the interaction of TcFHc and TcFHm with the two substrates further, assays were then performed in the presence of a fixed amount of parasite enzyme (10 μg) using different concentrations of fumarate/malate substrates (Table 1). This revealed that TcFHc catalysed the hydration and dehydration reactions following the Hill model with a Hill coefficient (h) of 1.4, with its catalytic efficiency ($k_{cat}/k_{0.5}^{h}$), calculated as suggested in [28], towards the hydration of fumarate: this reaction was six-fold greater than the dehydration of malate. In contrast, TcFHm follows the simpler Michaelis-Menten mechanism (h = 1) for both reaction directions, displaying a four-fold higher catalytic efficiency for malate formation. This indicates that *in vitro* both TcFHc and TcFHm have a preference for the hydration reaction (*i.e.* fumarate consumption).

3.3 Localization of the T. cruzi fumarases

When analysed using PSORTII, TcFHm was predicted to contain an amino terminal sequence with potential to target the enzyme to the parasite's single mitochondrion. To confirm this, versions of TcFHm tagged at its carboxyl termini with a 10-amino acid epitope from the human c-myc protein (protein designated TcFHm-9e10) or with GFP (designated as TcFHm-GFP) were expressed in *T.*

cruzi epimastigotes. Using parasites expressing TcFHm-9e10, the distribution of the recombinant protein was assessed following digitonin permeabilization (Figure 2A). This demonstrated that only soluble fractions obtained using ~~the~~ high concentrations of non-ionic detergent required for mitochondrial permeabilization were positive for tagged TcFHm. This subcellular location was confirmed using *T. cruzi* expressing TcFHm-GFP where the fluorescence signal was restricted to a lattice-like structure found throughout the cell, a pattern typical for trypanosomal proteins localized to the large single mitochondrion (Figure 2B). To confirm this, cells were co-stained with the mitochondrial dye, MitoTracker. When the images were superimposed, the pattern of colocalization indicated that TcFHm-GFP was located in the same compartment as MitoTracker. When the fluorescence studies were extended to investigate TcFHc localization, a GFP signal throughout the whole cell was observed indicating this fumarase has a cytosolic localization (Figure 2C).

3.4 Functional studies on T. cruzi fumarases

To investigate the importance of the fumarase repertoire to *T. cruzi* a reverse genetic approach was used. DNA fragments corresponding to the 5′ and 3' regions of Tc*fhc* were cloned either side of a cassette containing blasticidin or puromycin resistance markers. These were then linearized and transfected in *T. cruzi* epimastigotes to construct heterozyote (Tc*fhc*$^{+/}$) and null mutant (Tc*fhcΔ*) parasite lines. Southern hybridisation was used to confirm that each integration event had occurred and demonstrated that both copies of the full length Tc*fhc* gene could readily be deleted from the parasite genome (Figure 3A and C). As lack of TcFHc had no effect on trypanosome growth and had no effect on the trypanosomes ability to infect and grow within mammalian cells (Figure 3F), by inference the cytosolic fumarase activity is non-essential for parasite growth under normal culture conditions. A similar strategy to interrupt both copies of the Tc*fhm* gene in the *T. cruzi* genome was employed resulting in construction of a Tc*fhm*$^{+/-}$ heterozygote and Tc*fhmΔ* null mutants (Figure 3B and D). By inference, TcFHm activity is non-essential for epimastigote growth under normal culture conditions. Intriguingly, when the growth of insect form epimastigote trypanosomes lacking TcFHm

was followed, the parasites failed to grow in the initial 48-h period exhibiting a pronounced lag phase (Figure 3E). Additionally, when mammalian cells were infected with *T. cruzi* Tc*fhmΔ* mutants and the parasites cultured as intracellular amastigotes, the trypanosome abundance load per host cell was ~3-fold lower than wild type (Figure 3F). This indicates that trypanosomes lacking TcFHm are less infective than parental parasites or that amastigote growth of the null line inside tissue cultured mammalian cell is somehow compromised.

To evaluate whether the combined fumarase activity is essential for parasite viability, attempts to interrupt both genes within a single cell to generate a Tc*fhcΔ* Tc*fhmΔ* double null mutant were initiated; in these experiments the Tc*fhm* puromycin-based integration constructs was modified such that resistance gene was replaced with sequences encoding for neomycin or hygromycin B phosphotransferase. The *neo*-containing Tc*fhm* integration cassette was linearized and transformed into *T. cruzi* Tc*fhcΔ* cells and a Tc*fhc* null mutant/Tc*fhm* heterozygote (Tc*fhcΔ* Tc*fhm*$^{+/-}$) line selected. Southern hybridisation was used to confirm correct integration of each gene disruption event (lane 5 Figure 3C and D). When the ability of Tc*fhcΔ* Tc*fhm*$^{+/-}$ line to infect and grow inside mammalian cells was monitored, the recombinant parasites behaved similarly to wild type and Tc*fhcΔ* lines (Figure 3F). Attempts to generate a Tc*fhcΔ* Tc*fhmΔ* double null mutant line using the hygromycin-based vector failed, leading us to speculate that the combined TcFHc and TcFHm activity is essential for epimastigote growth under normal culture conditions. Unfortunately, rescue experiments could not be undertaken as the gene interruption experiments outlined above exhausted all the selectable markers available for use in *T. cruzi*.

3.5 Developing a fumarase inhibitor

The gene disruption experiments suggest that the total fumarase activity may be essential for parasite viability. Encouraged by these observations, we became interested in evaluating this enzyme

repertoire as a potential drug target and investigating whether inhibitors specifically targeting class I fumarases could be developed.

The mechanism of substrate binding to the iron-sulfur cluster was previously proposed by Flint [23] and suggests that both the hydroxyl group of the substrate malate and one oxygen of the closest carboxylate are responsible for chelating the labile iron of the 4Fe-4S cluster and allowing the reaction to occur (Figure 4A). According to the hard soft (Lewis) acid base theory [29], the iron atoms of the cluster act as soft acids known to coordinate to thiol groups which are soft bases. Therefore, the chemistry of iron-sulfur clusters suggested to us that the replacement of a hydroxyl group (hard base) of L-malate with a thiol, as observed in the thiomalate molecule (Figure 4B), could potentialize the binding with the active site iron-sulfur cluster and block the enzyme activity.

To test this hypothesis, parasite fumarase (10 μg) activity was measured in the presence of different concentrations of malate (8, 4, 2, 1, and 0.5 mM) and thiomalate (12.86, 4.5, 1.58, 0.55 and 0 μM for TcFHc – Figure 4C) and (500, 250, 125, 62.5, 31.25, 15.62, 7.81, 3.91, 1.95, 0.98, 0.49, 0.24, 0.12, 0.061, 0.015 and 0 μM for TcFHm – Figure 4D). Under the conditions employed, thiomalate functioned as a competitive inhibitor of TcFHc and TcFHm dehydration reaction yielding Ki values of 4.2 ± 0.5 μM and 4.2 ± 0.5 μM, respectively. Since class II fumarases use an interaction network for catalysis that only involves residues and no metal (Figure 5A), we expected thiomalate to be selective towards class I fumarases. In fact, thiomalate did not affect the activity of purified class II human fumarase (Figure 5B).

When the inhibition studies were extended to investigate other thiol-based compounds, most (BME, Cys, GSH, DTT) had no significant effect on TcFHc activity even at high concentrations (>10 mM), with only DMSA having an inhibitory effect at concentrations below 2 mM (Figure 4E).

4. Discussion

Fumarases represent a class of metabolic enzymes expressed by many prokaryotic and eukaryotic cells where they play key roles in pathways as diverse as the TCA cycle, amino acid metabolism and DNA repair [12]. Their importance in humans is manifest when the encoded activity becomes compromised such that reduction in fumarase levels can lead to a series of neonatal and infantile neurological conditions as well as in promoting certain cancers [30, 31]. Here, we demonstrate that *T. cruzi* expresses two *bona fide* [4Fe-4S] cluster-containing fumarases that within the parasites cytosol or mitochondrion mediate the interconversion of fumarate and malate. Our data also suggest that their combined activities is essential for parasite growth, thereby genetically validating this enzyme repertoire as a drug target. Thus, the design a molecule to inhibit only the *T. cruzi* fumarases and not the human enzyme may be considered an attractive strategy for the development of new anti-chagasic compounds.

Based on their sequences, TcFHc and TcFHm display characteristics of the class I fumarases as expressed by bacteria and lower eukaryotes, possessing the fumarase (pfam05681) and fumarase C-terminus (pfam05683) domains that mediate [4Fe-4S] cluster co-factor binding. To confirm these computational observations recombinant versions of both enzymes were purified under anaerobic conditions following heterologous expression in *E.coli* and their kinetic properties analyzed. Initial assays demonstrated that TcFHc and TcFHm could catalyse the reversible conversion of fumarate and malate. As with the related *E. coli* fumA [23] and aconitase [32], the activity of both parasite enzymes was exquisitely sensitive to oxygen with as little as 20 ppm oxygen promoting conversion of the [4Fe-4S] to an [3Fe-4S] cluster, with loss of the labile iron leading to their irreversible deactivation. More detailed analysis on the kinetic properties of the trypanosomal fumarases revealed that whereas TcFHm was shown to exhibit Michaelis-Menten kinetics for both reaction directions

over the substrate concentration range tested (Table 1), TcFHc employed a catalytic mechanism with positive cooperativity, in agreement with its dimeric quaternary structure [33]. Since this profile was observed for both fumarate and malate, the interference of an optically impure substrate can be ruled out considering that fumarate is not a chiral molecule.

The localization of TcFHc to the cytosol and TcFHm to the mitochondrion as shown experimentally is in agreement with *in silico* predictions using Mitoprot [34] and experimental reports for the *T. brucei* and *L. major* homologues [15, 35]. However, computation analysis also indicates that TcFHc and TcFHm may also be present in glycosomes: glycosomes are modified peroxisomes within which several enzymes of the glycolytic pathway are compartmentalized. For TcFHc this additional localization, if ever exist, could be due to the presence of the –SKLL sequence at its carboxyl terminus, a region that resembles a classical peroxisomal targeting signal 1 (PTS1) (-SKL) tripeptide motif. What actually constitutes a PTS1 in glycosomes appears to be less stringent than for peroxisomes [36-39]. Although structural studies involving *T. brucei* PEX5, the receptor that initiates protein translocation into the glycosome, in complex with modified PTS1 sequences has revealed that the extra leucine added onto the SKL-like tripeptide would occupy an unfavorable highly polar cavity which is actually filled by a 1,2-ethanediol molecule what would probably hinder the protein-transporter interaction [40]. As TcFHc contains this tetrapeptide arrangement at its carboxyl terminal it may not be recognized by the glycosomal transport machinery. In the case of TcFHm its amino terminal contains a mitochondrial signal peptide (MLRRSAA-) closely followed by an internal peroxisomal targeting signal 2 (PTS2) (-KYVPLIPHV-), an arrangement also noted for the *L. major* and *T. brucei* orthologs [41]. Using a combination of approaches we clearly show that carboxy terminal tagged versions of this fumarase are only present in the parasite's single mitochondrion and at no other sites within the cell.

The endogenous function of each individual *T. cruzi* fumarase is non-essential to *T. cruzi*: both copies of Tc*fhc* or Tc*fhm* could be readily deleted from the genome of epimastigote parasites. For

trypanosomes lacking the cytosolic fumarase no obvious phenotype was observed with the recombinant parasites growing as insect form epimastigotes, invading mammalian cells as trypomastigotes or proliferating as intracellular amastigotes at levels equivalent to controls (Figure 3F). In contrast, deletion of both Tc*fhm* gene copies from the *T. cruzi* genome hampered the parasites ability to proliferate in its epimastigote and amastigote forms. As TcFHm most likely participates in the Kreb's cycle lack of its activity may alter the flux of metabolites within this pathway having a knock on effect in other biological systems such as in energy production and amino acid biosynthesis. Because the mitochondrial enzyme is not essential for parasite growth it is implicit that its activity can be complemented possibly indicating that *T. cruzi* may have the ability to shuttle malate and fumarate between cellular compartments [22] (this may also explain why the cytosolic fumarase is non-essential) or that the TcFHm deficient cells are able to undergo some type of biochemical adaptation and metabolic reprogramming, analogous to leiomyomatosis renal carcinoma cells that are null for fumarase [42].

The importance of the total fumarase activity to *T. cruzi* became evident when attempts were made to generate parasites lacking both genes. Here, three out of four fumarase gene alleles could readily be disrupted in epimastigote form trypanosomes with failure to interrupt the final gene strongly suggesting that the total fumarase activity is essential for parasite viability. Addition of malate or fumarate to the medium, a technique used to rescue for the fumarase knockdown phenotype in *T. brucei* [15], failed to generate the desired Tc*fhcΔ* Tc*fhmΔ* lines. The inability to complement for fumarase activity deficiency through supplementation of the medium with exogenous dicarboxylate indicates that *T. cruzi* epimastigotes may lack fumarate and malate transporters that facilitate their uptake into the cell.

Based on their biochemical features and apparent essential activity the *T. cruzi* fumarase repertoire possess many hallmarks required in a druggable target. To further assess whether these enzymes fulfil

other criterion required for chemotherapeutic development, an assay for specific class I fumarases inhibitors was undertaken with thiomalate, a chemical rationally selected based on its similarity to the malate/fumarate substrates and low toxicity to humans [43]. Assays revealed that this structure could readily inhibit the trypanosomal fumarase activity without significantly affecting the human enzyme *via* a mechanism postulated to involve thiomalate selectively binding to the iron-sulfur cluster, a co-factor absent from HsFH [44] (Figure 4A). Thiomalate therefore represents a novel chemical lead that because of its low lipophilicity will require derivatization in order to develop more bioavailable variants that can be used against intracellular pathogens such as *T. cruzi*.

Our work has demonstrated that the *T. cruzi* fumarase complement should be investigated as a potential druggable anti-chagasic target and has resulted in the identification of a lead structure in the form of thiomalate. As several other medically important protozoan parasites including *Plasmodium falciparum, Cryptosporidium* and *Leishmania* also express class I fumarases then the work reported here may facilitate the development of novel strategies towards the development of new treatments for a range of globally important pathogens.

5. Acknowledgments

This work received financial support from Fundação de Amparo a Pesquisa do Estado de São Paulo [FAPESP, Grants number 2008/08262-6 (MCN) and 2008/11644-8 (RAPP)] and from CAPES [Grant number BEX 1096/11-7 (RAPP)].

We would like to thank John Kelly and Martin Taylor (both LSHTM) for advice regarding generation of recombinant *T. cruzi* lines; Ana Patrícia Yatsuda Natsui, Maraísa Palhão Verri, Sérgio de Albuquerque and Cristiana Gonçalez for *T. cruzi* amastigote culture and imaging; Paul Michels and Frédéric Bringaud for the antibodies; and Patrícia Feliciano and Valquiria Jabor for their help in enzyme kinetics.

6. References

[1] G. Punukollu, R.A. Gowda, I.A. Khan, V.S. Navarro, B.C. Vasavada, Clinical aspects of the Chagas' heart disease, International Journal of Cardiology, 115 (2007) 279-283.
[2] B.A. Burleigh, N.W. Andrews, THE MECHANISMS OF TRYPANOSOMA-CRUZI INVASION OF MAMMALIAN-CELLS, Annual Review of Microbiology, 49 (1995) 175-200.
[3] K.S. Pereira, F.L. Sciimidt, A.M.A. Guaraldo, R.M.B. Franco, V.L. Dias, L.A.C. Passos, Chagas' Disease as a Foodborne Illness, Journal of Food Protection, 72 (2009) 441-446.
[4] D.V. Andrade, K.J. Gollob, W.O. Dutra, Acute Chagas Disease: New Global Challenges for an Old Neglected Disease, Plos Neglected Tropical Diseases, 8 (2014).
[5] S.K. Burley, F. Park, Meeting the challenges of drug discovery: a multidisciplinary re-evaluation of current practices, Genome Biology, 6 (2005).
[6] H.D. Dakin, The action of muscle tissue on fumaric, maleic, glutaconic, and malic acids, Journal of Biological Chemistry, 52 (1922) 183-189.
[7] S.A. Woods, S.D. Schwartzbach, J.R. Guest, 2 BIOCHEMICALLY DISTINCT CLASSES OF FUMARASE IN ESCHERICHIA-COLI, Biochimica Et Biophysica Acta, 954 (1988) 14-26.
[8] J.R. Guest, J.S. Miles, R.E. Roberts, S.A. Woods, THE FUMARASE GENES OF ESCHERICHIA-COLI - LOCATION OF THE FUMB GENE AND DISCOVERY OF A NEW GENE (FUMC), Journal of General Microbiology, 131 (1985) 2971-2984.
[9] O. Yogev, A. Naamati, O. Pines, Fumarase: a paradigm of dual targeting and dual localized functions, Febs Journal, 278 (2011) 4230-4242.
[10] E. Burak, O. Yogev, S. Sheffer, O. Schueler-Furman, O. Pines, Evolving Dual Targeting of a Prokaryotic Protein in Yeast, Molecular Biology and Evolution, 30 (2013) 1563-1573.
[11] O. Yogev, O. Pines, Dual targeting of mitochondrial proteins: Mechanism, regulation and function, Biochimica Et Biophysica Acta-Biomembranes, 1808 (2011) 1012-1020.
[12] O. Yogev, E. Singer, E. Shaulian, M. Goldberg, T.D. Fox, O. Pines, Fumarase: A Mitochondrial Metabolic Enzyme and a Cytosolic/Nuclear Component of the DNA Damage Response, Plos Biology, 8 (2010).
[13] B.L.M. VanKuijk, N.D. VanLoo, A.F. Arendsen, W.R. Hagen, A.J.M. Stams, Purification and characterization of fumarase from the syntrophic propionate-oxidizing bacterium strain MPOB, Archives of Microbiology, 165 (1996) 126-131.
[14] T. Shimoyama, E. Rajashekhara, D. Ohmori, T. Kosaka, K. Watanabe, MmcBC in Pelotomaculum thermopropionicum represents a novel group of prokaryotic fumarases, Fems Microbiology Letters, 270 (2007) 207-213.
[15] V. Coustou, M. Biran, S. Besteiro, L. Riviere, T. Baltz, J.M. Franconi, F. Bringaud, Fumarate is an essential intermediary metabolite produced by the procyclic Trypanosoma brucei, Journal of Biological Chemistry, 281 (2006) 26832-26846.
[16] M. Navarro, N. De, N. Bae, Q. Wang, H. Sondermann, Structural Analysis of the GGDEF-EAL Domain-Containing c-di-GMP Receptor FimX, Structure, 17 (2009) 1104-1116.
[17] R.A. Pereira de Padua, M.C. Nonato, Cloning, expression, purification, crystallization and preliminary X-ray diffraction analysis of recombinant human fumarase, Acta Crystallographica Section F-Structural Biology and Crystallization Communications, 70 (2014) 120-122.
[18] R.M. Bock, R.A. Alberty, STUDIES OF THE ENZYME FUMARASE .1. KINETICS AND EQUILIBRIUM, Journal of the American Chemical Society, 75 (1953) 1921-1925.
[19] E. Nakamaru-Ogiso, T. Yano, T. Ohnishi, T. Yagi, Characterization of the iron-sulfur cluster coordinated by a cysteine cluster motif (CXXCXXXCX27C) in the Nqo3 subunit in the proton-

translocating NADH-quinone oxidoreductase (NDH-1) of Thermus thermophilus HB-8, Journal of Biological Chemistry, 277 (2002) 1680-1688.
[20] A. Maria Mejia, B.S. Hall, M.C. Taylor, A. Gomez-Palacio, S.R. Wilkinson, O. Triana-Chavez, J.M. Kelly, Benznidazole-Resistance in Trypanosoma cruzi Is a Readily Acquired Trait That Can Arise Independently in a Single Population, Journal of Infectious Diseases, 206 (2012) 220-228.
[21] S.M. Wilkinson, D.J. Meyer, M.C. Taylor, E.V. Bromley, M.A. Miles, J.M. Kelly, The Trypanosoma cruzi enzyme TcGPXI is a glycosomal peroxidase and can be linked to trypanothione reduction by glutathione or tryparedoxin, Journal of Biological Chemistry, 277 (2002) 17062-17071.
[22] M. Aslett, C. Aurrecoechea, M. Berriman, J. Brestelli, B.P. Brunk, M. Carrington, D.P. Depledge, S. Fischer, B. Gajria, X. Gao, M.J. Gardner, A. Gingle, G. Grant, O.S. Harb, M. Heiges, C. Hertz-Fowler, R. Houston, F. Innamorato, J. Iodice, J.C. Kissinger, E. Kraemer, W. Li, F.J. Logan, J.A. Miller, S. Mitra, P.J. Myler, V. Nayak, C. Pennington, I. Phan, D.F. Pinney, G. Ramasamy, M.B. Rogers, D.S. Roos, C. Ross, D. Sivam, D.F. Smith, G. Srinivasamoorthy, C.J. Stoeckert, Jr., S. Subramanian, R. Thibodeau, A. Tivey, C. Treatman, G. Velarde, H. Wang, TriTrypDB: a functional genomic resource for the Trypanosomatidae, Nucleic Acids Research, 38 (2010) D457-D462.
[23] D.H. Flint, M.H. Emptage, J.R. Guest, FUMARASE-A FROM ESCHERICHIA-COLI - PURIFICATION AND CHARACTERIZATION AS AN IRON SULFUR CLUSTER CONTAINING ENZYME, Biochemistry, 31 (1992) 10331-10337.
[24] J. Telser, H.I. Lee, B.M. Hoffman, Investigation of exchange couplings in Fe3S4 (+) clusters by electron spin-lattice relaxation, Journal of Biological Inorganic Chemistry, 5 (2000) 369-380.
[25] N.M. Brown, M.C. Kennedy, W.E. Antholine, R.S. Eisenstein, W.E. Walden, Detection of a 3Fe-4S cluster intermediate of cytosolic aconitase in yeast expressing iron regulatory protein 1 - Insights into the mechanism of Fe-S cluster cycling, Journal of Biological Chemistry, 277 (2002) 7246-7254.
[26] D.M.H. Ossa, R.R. Oliveira, M.T. Murakami, R. Vicentini, A.J. Costa-Filho, F. Alexandrino, L.M.M. Ottoboni, O. Garcia Jr, Expression, purification and spectroscopic analysis of an HdrC: An iron-sulfur cluster-containing protein from Acidithiobacillus ferrooxidans, Process Biochemistry, 46 (2011) 1335-1341.
[27] B.M.A. van Vugt-Lussenburg, L. van der Weel, W.R. Hagen, P.L. Hagedoorn, Identification of two 4Fe-4S -cluster-containing hydro-lyases from Pyrococcus furiosus, Microbiology-Sgm, 155 (2009) 3015-3020.
[28] A. Cornish-Bowden, M.L. Cardenas, Specificity of Non-Michaelis-Menten Enzymes: Necessary Information for Analyzing Metabolic Pathways, Journal of Physical Chemistry B, 114 (2010) 16209-16213.
[29] R.G. Pearson, HARD AND SOFT ACIDS AND BASES, Journal of the American Chemical Society, 85 (1963) 3533-&.
[30] C. Ewbank, J.F. Kerrigan, K. Aleck, Fumarate Hydratase Deficiency, in: R.A. Pagon, M.P. Adam, H.H. Ardinger, S.E. Wallace, A. Amemiya, L.J. Bean, T.D. Bird, C.-T. Fong, H.C. Mefford, R.J. Smith, K. Stephens (Eds.) Gene reviews, University of Washington, Seattle, 2006 Jul 5 [Updated 2013 Apr 4].
[31] P.J. Ratcliffe, Fumarate hydratase deficiency and cancer: Activation of hypoxia signaling?, Cancer Cell, 11 (2007) 303-305.
[32] A.H. Robbins, C.D. Stout, IRON-SULFUR CLUSTER IN ACONITASE - CRYSTALLOGRAPHIC EVIDENCE FOR A 3-IRON CENTER, Journal of Biological Chemistry, 260 (1985) 2328-2333.
[33] H. Prinz, A. Schönichen, Transient binding patches: a plausible concept for drug binding, Journal of Chemical Biology, 1 (2008) 95-104.
[34] M.G. Claros, P. Vincens, Computational method to predict mitochondrially imported proteins and their targeting sequences, European Journal of Biochemistry, 241 (1996) 779-786.

[35] P.R. Feliciano, S. Gupta, F. Dyszy, M. Dias-Baruffi, A.J. Costa-Filho, P.A.M. Michels, M.C. Nonato, Fumarate hydratase isoforms of Leishmania major: Subcellular localization, structural and kinetic properties, International journal of biological macromolecules, 51 (2012) 25-31.
[36] P.E. Purdue, P.B. Lazarow, Targeting of human catalase to peroxisomes is dependent upon a novel COOH-terminal peroxisomal targeting sequence, Journal of Cell Biology, 134 (1996) 849-862.
[37] C. Brocard, A. Hartig, Peroxisome targeting signal 1: Is it really a simple tripeptide?, Biochimica Et Biophysica Acta-Molecular Cell Research, 1763 (2006) 1565-1573.
[38] J.M. Sommer, C.C. Wang, TARGETING PROTEINS TO THE GLYCOSOMES OF AFRICAN TRYPANOSOMES, Annual Review of Microbiology, 48 (1994) 105-138.
[39] F. Duffieux, J. Van Roy, P.K.M. Michels, F.R. Opperdoes, Molecular characterization of the first two enzymes of the pentose-phosphate pathway of Trypanosoma brucei - Glucose-6-phosphate dehydrogenase and 6-phosphogluconolactonase, Journal of Biological Chemistry, 275 (2000) 27559-27565.
[40] P. Sampathkumar, C. Roach, P.A.M. Michels, W.G.J. Hol, Structural insights into the recognition of peroxisomal targeting signal 1 by Trypanosoma brucei peroxin 5, Journal of Molecular Biology, 381 (2008) 867-880.
[41] F.R. Opperdoes, J.P. Szikora, In silico prediction of the glycosomal enzymes of Leishmania major and trypanosomes, Molecular and Biochemical Parasitology, 147 (2006) 193-206.
[42] Y. Yang, A.N. Lane, C.J. Ricketts, C. Sourbier, M.-H. Wei, B. Shuch, L. Pike, M. Wu, T.A. Rouault, L.G. Boros, T.W.M. Fan, W.M. Linehan, Metabolic Reprogramming for Producing Energy and Reducing Power in Fumarate Hydratase Null Cells from Hereditary Leiomyomatosis Renal Cell Carcinoma, Plos One, 8 (2013).
[43] S.R. Rudge, D. Perrett, A.J. Swannell, FREE THIOMALATE IN PLASMA AND URINE OF PATIENTS RECEIVING SODIUM AUROTHIOMALATE, Annals of the Rheumatic Diseases, 43 (1984) 66-69.
[44] M. Estevez, J. Skarda, J. Spencer, L. Banaszak, T.M. Weaver, X-ray crystallographic and kinetic correlation of a clinically observed human fumarase mutation, Protein Science, 11 (2002) 1552-1557.
[45] R.W. Miller, C.T. Kerr, J.R. Curry, Fumarase A from *Escherichia coli*: purification and characterization as an iron-sulfur cluster containing enzymeMAMMALIAN DIHYDROOROTATE-UBIQUINONE REDUCTASE COMPLEX, Canadian Journal of Biochemistry, 46 (1968) 1099-&.

TABLE

Table 1. Kinetic parameters of *T. cruzi* fumarases. TcFHc and TcFHm kinetic parameters were obtained for the L-malate and fumarate substrates under anaerobic conditions. Initial rates were plotted versus substrate concentration and the data fitted to Hill model. Enzyme concentration was determined by absorbance of [4Fe-4S] cluster at 410 nm (ε_{410nm}=15000 $M^{-1}.cm^{-1}$). k_{cat} is the enzyme turnover number, h is the Hill coefficient, $k_{0.5}$ is the substrate concentration at half maximum velocity when $h \neq 1$, k_m is the substrate concentration at half maximum velocity when $h = 1$, $k_{cat}/k_{0.5}^{h}$ and k_{cat}/k_m are the enzyme catalytic efficiencies for a given substrate and R^2 is the adjusted coefficient of determination.

	Substrate	k_{cat} (s^{-1})	k_m (M)	$k_{0.5}$ (M)	Hill coeff. (h)	$k_{cat}/k_{0.5}^{h}$ ($s^{-1}.M^{-1.4}$)	k_{cat}/k_m ($s^{-1}.M^{-1}$)	R^2
***Tc*FHc**	L-malate	290 ± 40	-	2.5 ± 0.6 x 10^{-3}	1.4 ± 0.1	1.3 x 10^6	-	99%
	fumarate	400 ± 100	-	0.8 ± 0.2 x 10^{-3}	1.4 ± 0.2	8.2 x 10^6	-	99%
***Tc*FHm**	L-malate	1050 ± 40	2.8 ± 0.2 x 10^{-3}		-	-	0.4 x 10^6	100%
	fumarate	2300 ± 500	1.5 ± 0.4 x 10^{-3}		-	-	1.5 x 10^6	98%

FIGURE LEGENDS

FIGURE 1. Analysis of purified trypanosomal fumarases. A). Purified TcFHc (lane 1), TcFHm (lane 2) (upper band corresponding to unprocessed SUMO tag) and *Hs*FH (lane 3) (1 µg per enzyme) were fractionated by SDS-PAGE. B). Elution profile of DTT (1 mM) treated *Tc*FHc off a Superdex 300 column. C and D). EPR spectra of *T. cruzi* fumarases TcFHc (C) and TcFHm (D). Both spectra contain resonances centered in g ~ 2.019 which is considered a fingerprint of a $[3Fe\text{-}4S]^{+}$ cluster. This type of cluster in class I fumarases are generated after the oxidation of [4Fe-4S] cluster by oxygen.

FIGURE 2. Subcellular localization of *T. cruzi* fumarases: A). Digitonin permeabilization of *T. cruzi* cells expressing c-myc tagged TcFHm: TcFHm was released concomitantly with ASCT (mitochondrial marker) at high digitonin concentration, while the enzymes aldolase (glycosomal) and enolase (cytosolic) were released at lower digitonin concentrations. B and C). *T. cruzi* expressing GFP tagged TcFHm (B) or TcFHc (C) co-stained with DAPI (DNA) and/or Mitotracker (MT) were analyzed by confocal microscopy. The pattern of TcFHm-GFP and Mitotracker co-localization (yellow) is shown in the merged image indicating this trypanosomal enzyme is present in the parasites' single mitochondrion. For TcFHc-GFP, a signal throughout the whole cell was observed typical of cytosolic proteins.

FIGURE 3. Analysis of *T. cruzi* fumarases null mutant lines. A and B). Diagrams of the Tc*fhc* (A) and Tc*fhm* (B) alleles (both in light grey) and the effects of gene disruption. The fumarase encoding genes were interrupted using cassettes containing the puromycin (*pac*), blasticidin (*bla*) or neomycin (*neo*) selectable markers (dark grey) flanked by tubulin intergenic elements (hashed boxes) required for processing of mRNA. The dotted lines correspond to probes used to check integration. The position of the predicted *Nco*I (N) or *Xho*I (X) sites plus the band sizes (in kbp) obtained after hybridization are shown. C and D). Autoradiograph of *Nco*I- (C) or *Xho*I- (D) digested genomic DNA from *T. cruzi* Sylvio X10.6 wild type

(lane 1), Tc*fhc*$^{+/-BLA}$ or Tc*fhm*$^{+/-BLA}$ heterozygote (lane 2), Tc*fhc*$^{+/-PAC}$ or Tc*fhm*$^{+/-PAC}$ heterozygote (lane 3), Tc*fhc*Δ or Tc*fhm*Δ null mutant (lane 4) and Tc*fhc*Δ null mutant/Tc*fhm*$^{+/-NEO}$ heterozygote (lane 5) cell lines hybridized with labelled Tc*fhc* (panel C) or Tc*fhm* (panel D). The band sizes are in kbp. E). The growth of *T. cruzi* Sylvio X10.6 wild type (WT) (blue continuous line) and Tc*fhm*Δ null mutant (red dotted line) cells was monitored over a 20 day period. Each data point represents a mean ± standard deviation from cell counts performed on three independent cultures. F). *T. cruzi* Sylvio X10.6 wild type (WT), Tc*fhc*Δ or Tc*fhm*Δ null mutants and Tc*fhc*Δnull mutant/Tc*fhm*$^{+/-NEO}$ heterozygote lines were used to infect mammalian (Vero) cells. The number of infected cells and the number of amastigotes per mammalian cell were determined and the mean abundance of parasites per mammalian cell. Error bars represent the 95% confidence intervals calculated using the quantitative parasitology software QPweb 1.0. The figure to the left shows a mammalian cell infected with wild type *T. cruzi* Sylvio X10/6.

FIGURE 4. Inhibitor design for class I fumarase. A) The structure of aconitase in complex with isocitrate (PDB ID: 7ACN) was used as a guide for modeling the binding of malate to the iron sulfur cluster first proposed by Flint [45]. B) We hypothesized that replacing the hydroxyl group of malate by a thiol group would result in a strong interaction with the cluster, therefore inhibiting the enzyme. C) TcFHc activity was evaluated in the presence of different thiomalate concentrations. The data fitted a competitive inhibition model with Ki = 4.2 ± 0.5 μM. D) Inhibition of TcFHm by thiomalate was assessed and the data fitted a competive model E) The effect of various thiol containing compounds on TcFHc activity was assessed. β-mercaptoethanol (BME), cysteine (Cys), reduced glutathione (GSH) and dithiotreitol (DTT) only inhibited TcFHc when their concentrations were higher than that of L-malate concentration used (8 mM). Only meso-2,3-dimercaptosuccinate (DMSA) inhibited TcFHc activity suggesting that this molecule resembles the substrate to access the active site of class I fumarases.

FIGURE 5. Thiomalate is selective towards the parasite fumarase. A) The structures of the human fumarase (PDB ID: 3E04, green) and *Micobacterium tuberculosis* fumarase in complex with fumarate (PDB ID: 4APB, cyan) were superimposed to show that the binding of fumarate to class II fumarases relies only on residue interactions and is independent of iron. B) Thiomalate was also tested against *Hs*FH activity and inhibition only occurred when the concentrations of inhibitor and substrate were similar, which means thiomalate is a poor inhibitor for the human fumarase.

FIGURE 1

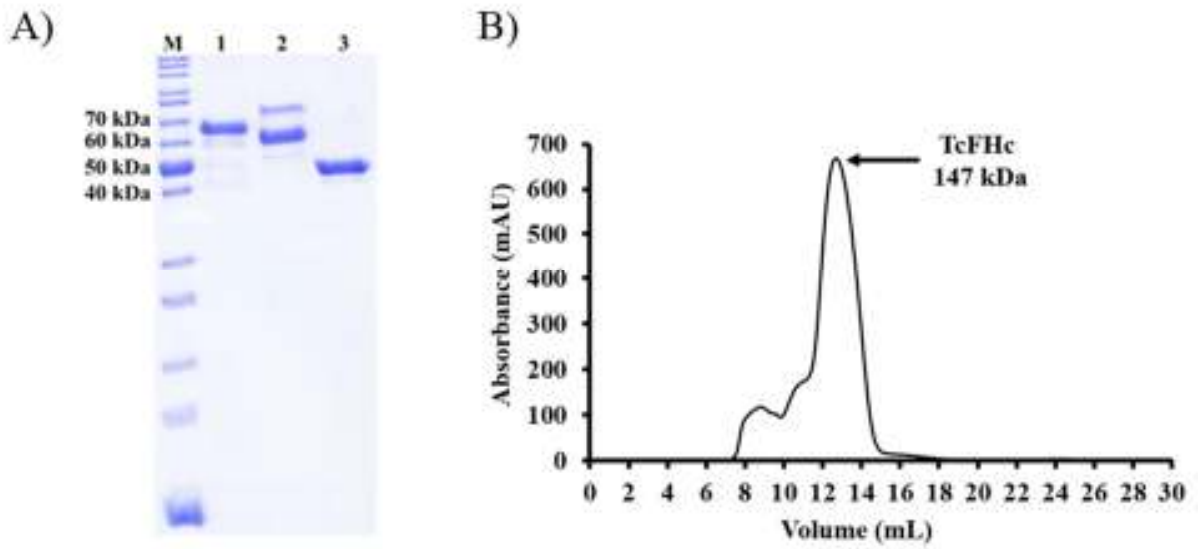
A)
M
1
2
3
70 kDa
60 kDa
50 kDa
40 kDa
B)
TcFHc
147 kDa
Absorbance (mAU)
Volume (mL)

C) D)

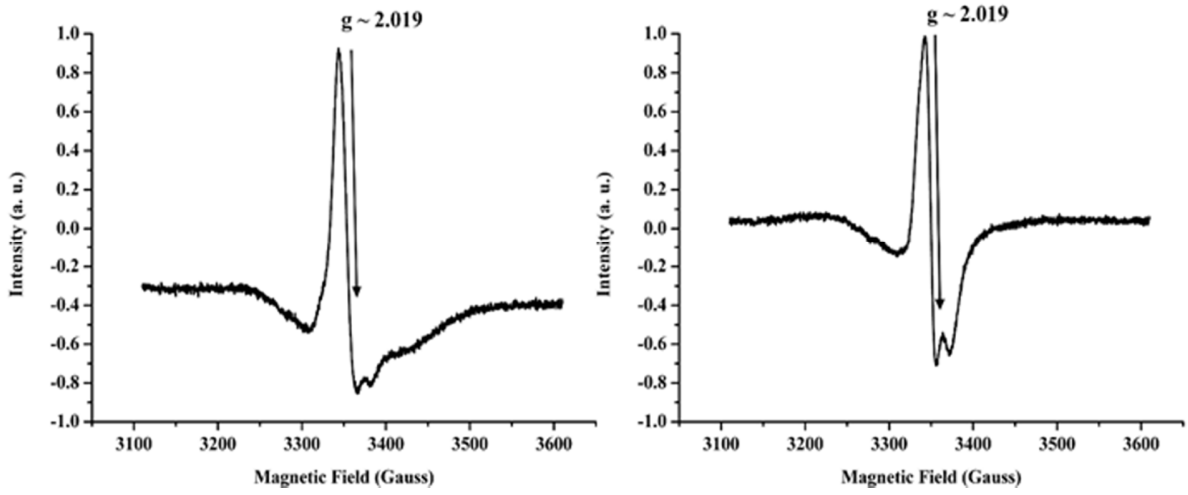
g ~ 2.019
Intensity (a. u.)
Magnetic Field (Gauss)
g ~ 2.019
Intensity (a. u.)
Magnetic Field (Gauss)

FIGURE 2

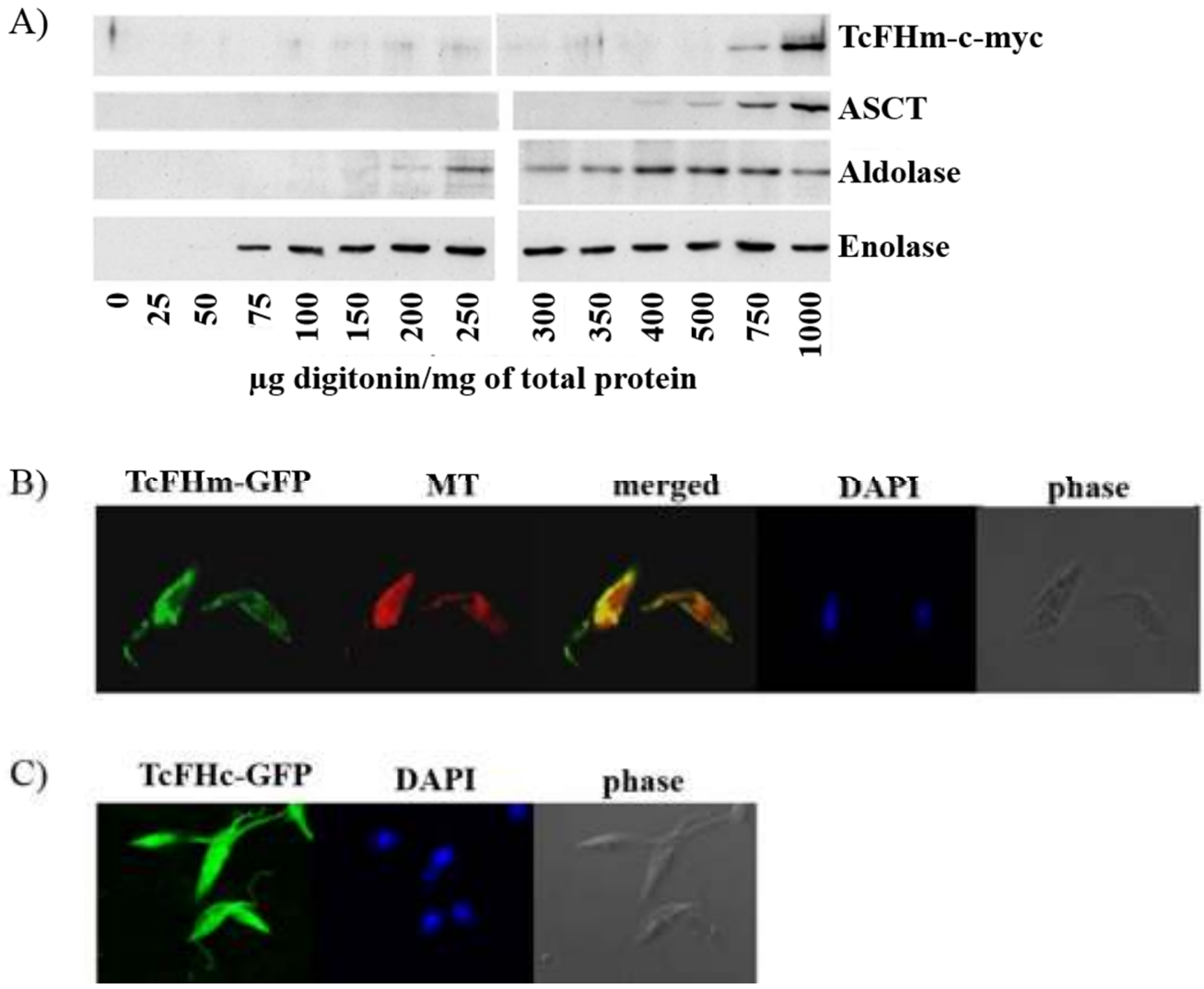
A)
TcFHm-c-myc
ASCT
Aldolase
Enolase
0
25
50
75
100
150
200
250
300
350
400
500
750
1000
µg digitonin/mg of total protein
B)
TcFHm-GFP
MT
merged
DAPI
phase
C)
TcFHc-GFP
DAPI
phase

FIGURE 3

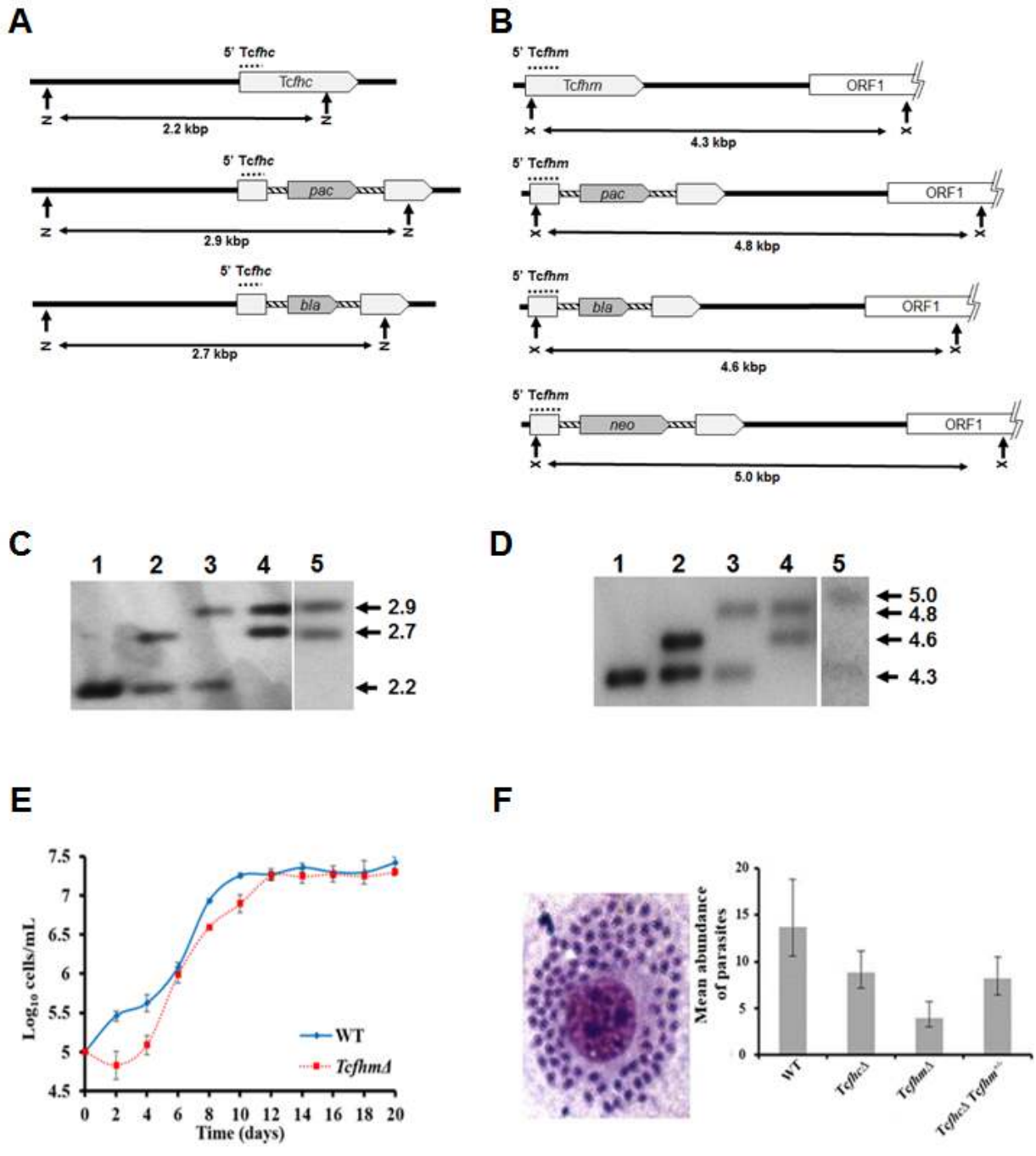
A
5' Tcfhc
Tcfhc
N
2.2 kbp
N
5' Tcfhc
pac
2.9 kbp
5' Tcfhc
bla
2.7 kbp
B
5' Tcfhm
Tcfhm
ORF1
X
4.3 kbp
5' Tcfhm
pac
4.8 kbp
5' Tcfhm
bla
4.6 kbp
5' Tcfhm
neo
5.0 kbp
C
1 2 3 4 5
2.9
2.7
2.2
D
1 2 3 4 5
5.0
4.8
4.6
4.3
E
Log10 cells/mL
Time (days)
WT
TcfhmΔ
F
Mean abundance of parasites
WT
Tcfhc∆
Tcfhm∆
Tcfhc∆ Tcfhm-/-

FIGURE 4

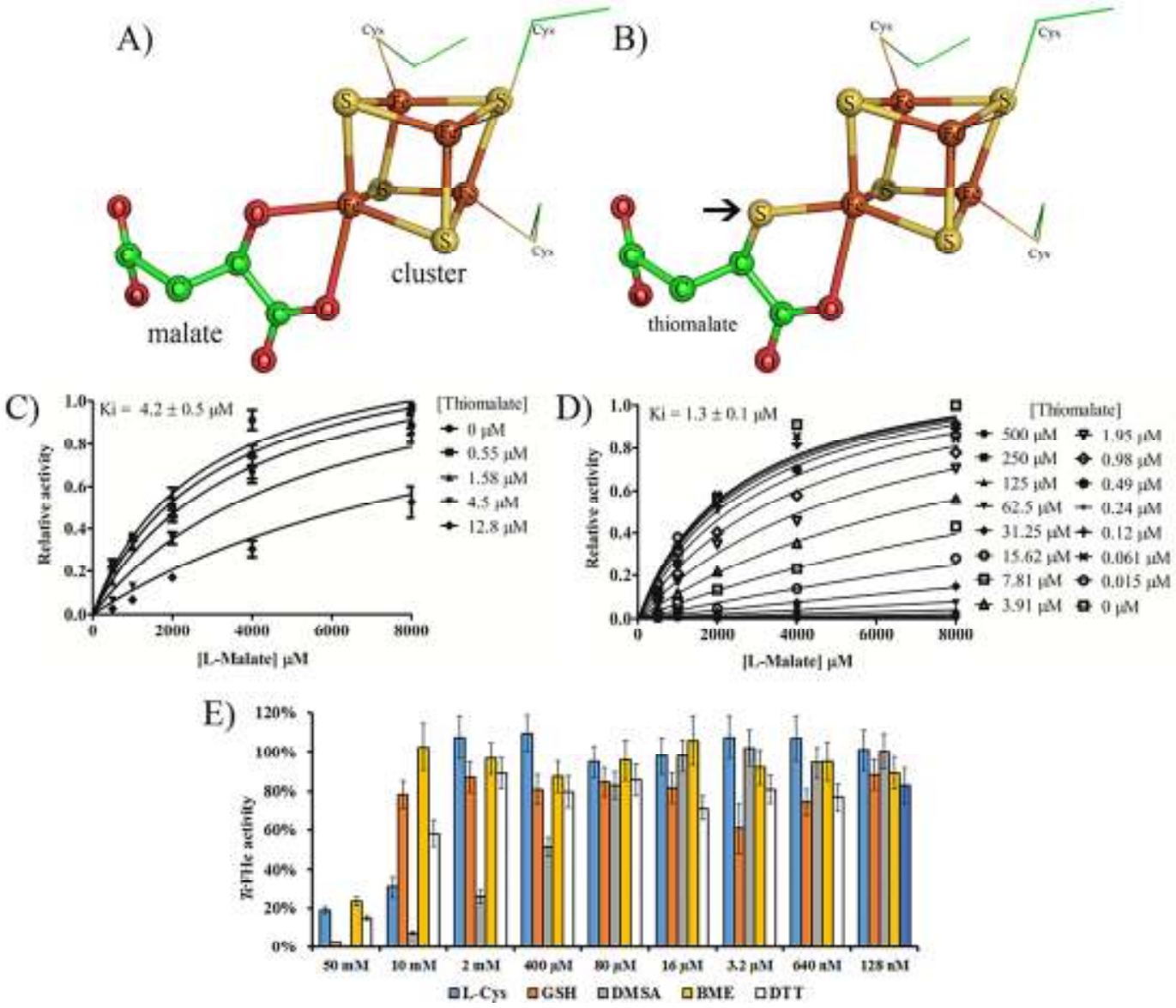
A)
Cys
Cys
S
Fe
S
Fe
S
Fe
S
Cys
cluster
malate
B)
Cys
Cys
S
Fe
S
Fe
S
Fe
S
Cys
thiomalate
C)
Ki = 4.2 ± 0.5 µM
Relative activity
[L-Malate] µM
[Thiomalate]
0 µM
0.55 µM
1.58 µM
4.5 µM
12.8 µM
D)
Ki = 1.3 ± 0.1 µM
Relative activity
[L-Malate] µM
[Thiomalate]
500 µM
250 µM
125 µM
62.5 µM
31.25 µM
15.62 µM
7.81 µM
3.91 µM
1.95 µM
0.98 µM
0.49 µM
0.24 µM
0.12 µM
0.061 µM
0.015 µM
0 µM
E)
TrTHc activity
50 mM
10 mM
2 mM
400 µM
80 µM
16 µM
3.2 µM
640 nM
128 nM
L-Cys
GSH
DMSA
BME
DTT

FIGURE 5

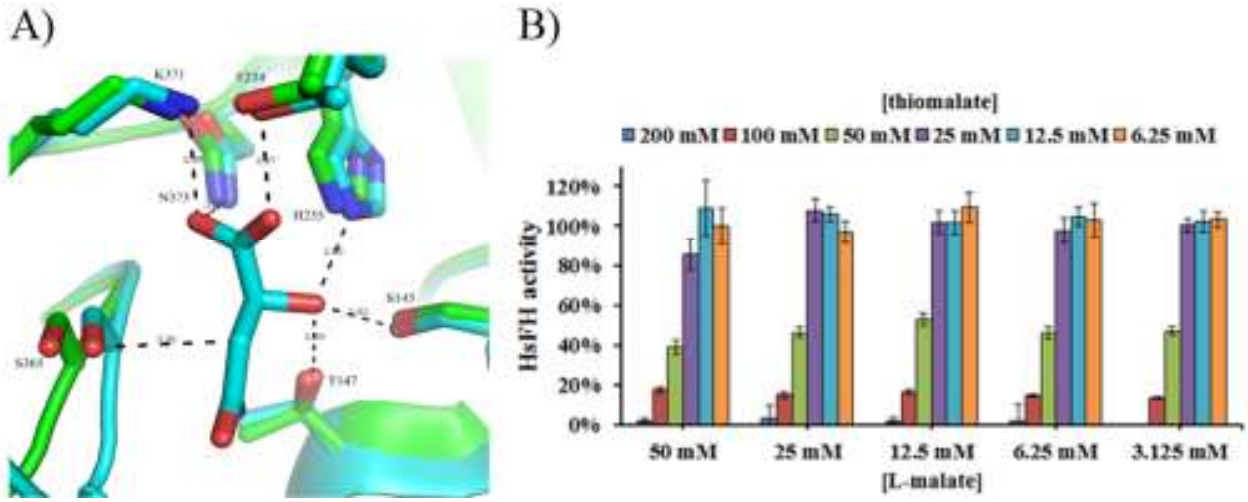
A)
B)
[thiomalate]
200 mM
100 mM
50 mM
25 mM
12.5 mM
6.25 mM
HslFH activity
120%
100%
80%
60%
40%
20%
0%
50 mM
25 mM
12.5 mM
6.25 mM
3.125 mM
[L-malate]